REFERENCES

1. Ichikawa T, Saito K, Yoshioka N, Tanimoto A, Gokan T, Takehara Y, et al. Detection and characterization of focal liver lesions: A Japanese phase III, multicenter comparison between gadoxetic acid disodium-enhanced magnetic resonance imaging and contrast-enhanced computed tomography predominantly in patients with hepatocellular carcinoma and chronic liver disease. Invest Radiol. 2010;45(3):133-41.

2. Halavaara J, Breuer J, Ayuso C, Balzer T, Bellin MF, Blomqvist L, et al. Liver tumor characterization: comparison between liver-specific gadoxetic acid disodium-enhanced MRI and biphasic CT--a multicenter trial. J Comput Assist Tomogr. 2006;30(3):345-54.

3. Hamm B, Staks T, Muhler A, Bollow M, Taupitz M, Frenzel T, et al. Phase I clinical evaluation of Gd-EOB-DTPA as a hepatobiliary MR contrast agent: safety, pharmacokinetics, and MR imaging. Radiology. 1995;195(3):785-92.

4. Hammerstingl R, Huppertz A, Breuer J, Balzer T, Blakeborough A, Carter R, et al. European EOB-study group. Diagnostic efficacy of gadoxetic acid (Primovist)-enhanced MRI and spiral CT for a therapeutic strategy: comparison with intraoperative and histopathologic findings in focal liver lesions. Eur Radiol. 2008;18(3):457-67.

5. Huppertz A, Balzer T, Blakeborough A, Breuer J, Giovagnoni A, Heinz-Peer G, et al. European EOB Study Group. Improved detection of focal liver lesions at MR imaging: multicenter comparison of gadoxetic acid-enhanced MR images with intraoperative findings. Radiology. 2004;230(1):266-75.

6. Di Martino M, Marin D, Guerrisi A, Baski M, Galati F, Rossi M, et al. Intraindividual comparison of gadoxetate disodium-enhanced MR imaging and 64-section multidetector CT in the detection of hepatocellular carcinoma in patients with cirrhosis. Radiology. 2010;256(3):806-16.

7. Inoue T, Kudo M, Komuta M, Hayaishi S, Ueda T, Takita M, et al. Assessment of Gd-EOB-DTPA-enhanced MRI for HCC and dysplastic nodules and comparison of detection sensitivity versus MDCT. J Gastroenterol. 2012;47(9):1036-47.

8. Golfieri R, Renzulli M, Lucidi V, Corcioni B, Trevisani F, Bolondi L. Contribution of the hepatobiliary phase of Gd-EOB-DTPA-enhanced MRI to dynamic MRI in the detection of hypovascular small (</= 2 cm) HCC in cirrhosis. Eur Radiol. 2011;21(6):1233-42.

9. Kumada T, Toyoda H, Tada T, Sone Y, Fujimori M, Ogawa S, et al. Evolution of hypointense hepatocellular nodules observed only in the hepatobiliary phase of gadoxetate disodium-enhanced MRI. AJR Am J Roentgenol. 2011;197(1):58-63.

10. Motosugi U, Ichikawa T, Sano K, Sou H, Onohara K, Muhi A, et al. Outcome of hypovascular hepatic nodules revealing no gadoxetic acid uptake in patients with chronic liver disease. J Magn Reson Imaging. 2011;34(1):88-94.

11. Kim YK, Lee WJ, Park MJ, Kim SH, Rhim H, Choi D. Hypovascular hypointense nodules on hepatobiliary phase gadoxetic acid-enhanced MR images in patients with cirrhosis: Potential of DW imaging in predicting progression to hypervascular HCC. Radiology. 2012;265(1):104-14.

12. Hyodo T, Murakami T, Imai Y, Okada M, Hori M, Kagawa Y, et al. Hypovascular nodules in patients with chronic liver disease: risk factors for development of hypervascular hepatocellular carcinoma. Radiology. 2013;266(2):480-90.

13. Bartolozzi C, Battaglia V, Bargellini I, Bozzi E, Campani D, Pollina LE, et al. Contrast-enhanced magnetic resonance imaging of 102 nodules in cirrhosis: correlation with histological findings on explanted livers. Abdom Imaging. 2013;38(2):290-6.

14. Golfieri R, Grazioli L, Orlando E, Dormi A, Lucidi V, Corcioni B, et al. Which is the best MRI marker of malignancy for atypical cirrhotic nodules: hypointensity in hepatobiliary phase alone or combined with other features? Classification after Gd-EOB-DTPA administration. J Magn Reson Imaging. 2012;36(3):648-57.

15. Sano K, Ichikawa T, Motosugi U, Sou H, Muhi AM, Matsuda M, et al. Imaging study of early hepatocellular carcinoma: usefulness of gadoxetic acid-enhanced MR imaging. Radiology. 2011;261(3):834-44.

16. Motosugi U. Hypovascular hypointense nodules on hepatocyte phase gadoxetic acid-enhanced MR images: Too early or too progressed to determine hypervascularity. Radiology. 2013;267(1):317-8.

17. Asayama Y, Yoshimitsu K, Nishihara Y, Irie H, Aishima S, Taketomi A, et al. Arterial blood supply of hepatocellular carcinoma and histologic grading: radiologic-pathologic correlation. AJR Am J Roentgenol. 2008;190(1):W28-34.

18. Motosugi U, Ichikawa T, Sou H, Sano K, Tominaga L, Kitamura T, et al. Liver parenchymal enhancement of hepatocyte-phase images in Gd-EOB-DTPA-enhanced MR imaging: which biological markers of the liver function affect the enhancement? J Magn Reson Imaging. 2009;30(5):1042-6.

19. Bruix J, Sherman M. American Association for the Study of Liver Diseases. Management of hepatocellular carcinoma: an update. Hepatology. 2011;53(3):1020-2.

20. Motosugi U, Ichikawa T, Araki T. Rules, roles, and room for discussion in gadoxetic acid-enhanced magnetic resonance liver imaging: current knowledge and future challenges. Magnetic Rsonance in Medical Sciences. 2013;12(3):161-75.

21. Kitao A, Zen Y, Matsui O, Gabata T, Kobayashi S, Koda W, et al. Hepatocellular carcinoma: signal intensity at gadoxetic acid-enhanced MR Imaging--correlation with molecular transporters and histopathologic features. Radiology. 2010;256(3):817-26.

22. Narita M, Hatano E, Arizono S, Miyagawa-Hayashino A, Isoda H, Kitamura K, et al. Expression of OATP1B3 determines uptake of Gd-EOB-DTPA in hepatocellular carcinoma. J Gastroenterol. 2009;44(7):793-8.

23. Nasu K, Kuroki Y, Tsukamoto T, Nakajima H, Mori K, Minami M. Diffusion-weighted imaging of surgically resected hepatocellular carcinoma: imaging characteristics and relationship among signal intensity, apparent diffusion coefficient, and histopathologic grade. American Journal of Roentgenology. 2009;193(2):438-44.

24. Degos F, Christidis C, Ganne-Carrie N, Farmachidi JP, Degott C, Guettier C, et al. Hepatitis C virus related cirrhosis: time to occurrence of hepatocellular carcinoma and death. Gut. 2000;47(1):131-6.

25. Tarao K, Rino Y, Ohkawa S, Shimizu A, Tamai S, Miyakawa K, et al. Association between high serum alanine aminotransferase levels and more rapid development and higher rates of incidence of hepatocellular carcinoma in patients with hepatitis C virus-associated cirrhosis. Cancer. 1999;86(4):589-95.

26. Ikeda K, Saitoh S, Suzuki Y, Kobayashi M, Tsubota A, Koida I, et al. Disease

progression and hepatocellular carcinogenesis in patients with chronic viral hepatitis: a prospective observation of 2215 patients. J Hepatol. 1998;28(6):930-8.

27. Ikeda K, Saitoh S, Koida I, Arase Y, Tsubota A, Chayama K, et al. A multivariate analysis of risk factors for hepatocellular carcinogenesis: a prospective observation of 795 patients with viral and alcoholic cirrhosis. Hepatology. 1993;18(1):47-53.

FIGURE LEGENDS

Figure 1. Patient inclusion criteria. "*De novo* HCC" is a typical HCC that developed at sites in which no nodules had been seen on the initial gadoxetic acid-enhanced MRI.

Figure 2. Cumulative incidence rates of typical HCC development in the non-clean and clean liver groups.

Figure 3. Cumulative incidence rates of typical HCC at sites in which no nodules had been seen on the initial gadoxetic acid-enhanced MRI, *i.e.* "*de novo* HCC".

Figure 4. Stratified analyses of the non-clean liver as a risk factor for typical HCC development.

Table 1. Baseline patient characteristics.

Characteristics	Total n = 127	Non-clean liver n = 18	Clean liver n = 109	p value
Age in years	65 (30-88)	68 (46-82)	64 (30-88)	0.15
Male/female	68/59	10/8	58/51	1.00
Non-cirrhosis/cirrhosis	59/68	6/12	53/56	0.31
HBV/HCV	26/101	5/13	21/88	0.53
Platelet count ($\times 10^9$/L)	122 (30-410)	102 (46-187)	125 (30-410)	0.07
ALT (IU/L)	32 (7-206)	32 (14-95)	32 (7-206)	0.97
γ-GTP (IU/L)	31 (9-305)	31 (13-258)	31 (9-305)	0.68
AFP (ng/mL)	4 (1-582)	8 (2-181)	4 (1-582)	0.19

Note: Continuous data are shown as medians (range).

Table 2. Variables that predict HCC development: univariate and multivariate analyses.

	Univariate		Multivariate	
Variables	Hazard ratio (95% CI)	p value	Hazard ratio (95% CI)	p value
Male	0.56 (0.29-1.95)	0.755		
Age (per year)	1.06 (1.00-1.12)	0.039	1.08 (1.01-1.16)	0.024
Cirrhosis	14.37 (1.90-108.44)	0.009	3.54 (0.37-33.77)	0.231
HCV (vs. HBV)	4.39 (0.58-33.17)	0.151		
Platelet count (per 10^{10}/L)	1.19 (1.06-1.33)	0.003	1.17 (1.03-1.35)	0.017
ALT (per IU/L)	1.00 (0.99-1.02)	0.423		
γ-GTP (per IU/L)	1.00 (0.99-1.01)	0.688		
AFP > 10 ng/mL	3.98 (1.47-10.77)	0.006	1.47 (0.49-4.33)	0.486
Non-clean liver	12.36 (4.68-32.61)	< 0.001	9.41 (3.47-25.46)	< 0.001

1

Fig. 1

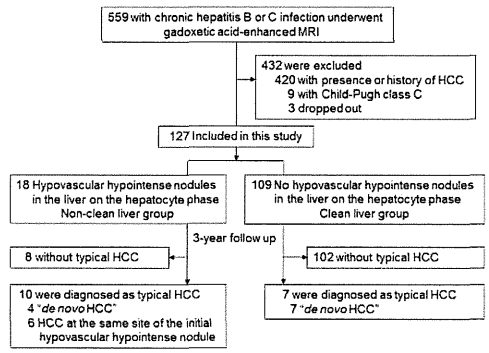

2

3 hepr_12309_f1

4

Fig. 2

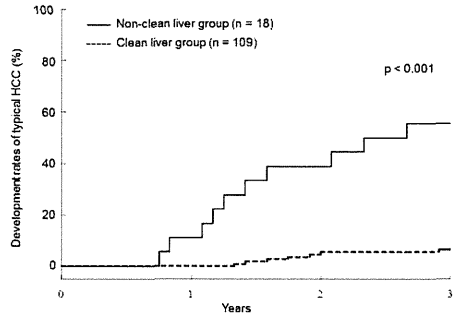

No. of patients at risk

Non-Clean liver	18	16	11	8
Clean liver	109	109	103	102

5

6 hepr_12309_f2

7

Fig. 3

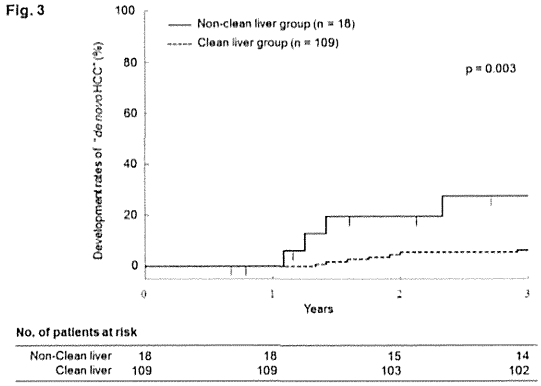

hepr_12309_f3

Fig. 4

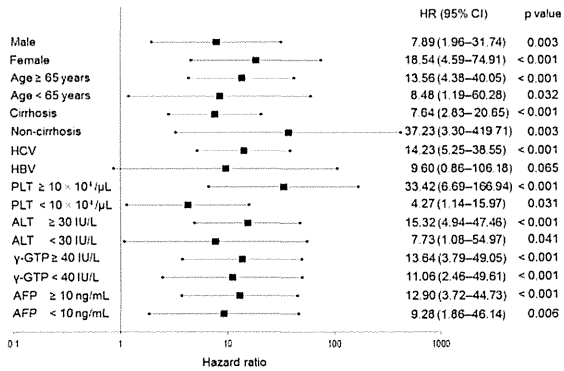

hepr_12309_f4

Design, Synthesis and Evaluation of Anti-HBV Activity of Hybrid Molecules of Entecavir and Adefovir: Exomethylene Acycloguanine Nucleosides and its Monophosphate Derivatives

Shuhei Imoto,[1)] Satoru Kohgo,[2,3)] Ryoh Tokuda,[1)] Hiroki Kumamoto,[4)] Manabu Aoki,[5)]

Masayuki Amano,[6)] Nobuyo Kuwata-Higashi,[6)] Hiroaki Mitsuya,[3,6,7)]

Kazuhiro Haraguchi[2)]*

1) Faculty of Pharmaceutical Sciences, Sojo University,

4-22-1 Ikeda, Nishi-ku, Kumamoto 860-0082, Japan

2) *Department of Pharmaceutical Sciences, Nihon Pharmaceutical University,*

10281 Komuro, Inamachi, Kita-adachi-gun, Saitama 362-0806, Japan

3) Center for Clinical Sciences, National Center for Global Health and Medicine,

1-21-1 Toyama, Shinju-ku, Tokyo 162-8655, Japan

4) School of Pharmacy, Showa University,

1-5-8 Hatanodai, Shinagawa-ku, Tokyo 142-8555, Japan

5) Department of Medical Technology, Kumamoto Heath Science University,

325 Izumimachi, Kumamoto 861-5598, Japan

6) Departments of Infectious Diseases and Hematology,

Kumamoto University School of Medicine, Kumamoto 860-8556, Japan

7) Experimental Retrovirology Section, HIV and AIDS Malignancy Branch,

National Cancer Institute, National Institutes of Health, Bethesda, MD, USA

Phone +81-48-721-7294

Fax +81-48-721-6718

harakazu@nichiyaku.ac.jp

Keywords: Nucleoside, Acyclonucleoside, Nucleoside phosphonate, Pro-drug, Hybrid, Entecavir, Adefovir, Anti-HBV activity

TOC GRAPHIC

Design, Synthesis and Evaluation of Anti-HBV Activity of Hybrid Molecules of Entecavir and Adefovir: Exomethylene Acycloguanine Nucleosides and its Monophosphate Derivatives

Shuhei Imoto, Satoru Kohgo, Ryoh Tokuda, Hiroki Kumamoto, Manabu Aoki, Masayuki Amano, Nobuyo Kuwata-Higashi, Hiroaki Mitsuya, Kazuhiro Haraguchi*

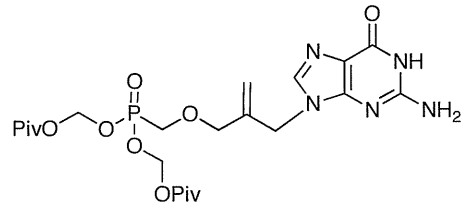

Piv-P-MEP-G

Abstract

Exomethylene acycloguanine nucleosides **4**, **6** and its monophosphate derivatives **5, 7** and **8** have been synthesized. Mitsunobu-type coupling of 2-*N*-acetyl-6-*O*-diphenylcarbamoylguanine (**11**) with the primary alcohols proceeded regioselectively to furnish the desired N^9-substituted products in moderate yield. Evaluation of **4-8** for anti-HBV activity in HepG2 cells revealed that the phosphonate derivative **8** was found to exhibit moderated activity (EC_{50} value of 0.29 μM) but cytotoxicity (CC_{50} value of 39 μM) against the host cells was also observed.

Introduction

Hepatitis B is one of the most prevalent viral diseases in the world and is known to be a major cause of chronic disease, leading to cirrhosis/hepatocellular carcinoma.[1] Among the most frequently used drugs for treatment of the disease,[2] are the nucleoside analogue entecavir (1)[3a,b] and the nucleotide analogue adefovir (2)[4] (Figure 1). Entecavir 1 is especially considered as one of the best choices for chronic patients due to its lack of significant adverse effects.[5] Entecavir is structurally a carbocyclic analogue of 2′-deoxyguanosine. The exomethylene functionality at the 5′-position of **1** would appear to be an important pharmacophore for the significant antiviral activity because the potency of carbocyclic dG that truncates the double bond is ten times less than that of **1**.[3a] In the meantime, adefovir **2** is the phosphonate analogue of the monophosphate of acycloadenine nucleoside. The feature of this class of nucleotide analogues is that the requisite first phosphorylation, which is a crucial step for the activation of biologically-active nucleoside derivatives, has been by-passed.

Further studies on the structure-activity relationship of these classes of nucleosides should increase our knowledge of the structural requirements for developing novel antiviral agents for HBV, and will aid in the search for better anti-HBV agents. In this context, we have envisioned combining the above two structural features in one

molecule and designed the exomethylene acyclic guanine nucleosides and its monophosphate derivatives as shown in Figure 2. The initial target molecules are exomethylene propyl- (**4**, MEP-G) and butyl- (**6**, MEB-G) guanine nucleosides. The number of constituted atoms (1′ to 4′-position) in the acyclic side chain of MEB-G **6** correspond to the structure consisting of C1′, C5′, C4′ and C7′ in entecavir **1** whereas MEP-G truncates one-carbon atom in the acyclic moiety. L-Ala-P-MEP-G **5** and L-Ala-P-MEB-G **7** are the respective phosphoalaninate pro-drugs of the monophophates of **4** and **6**. Moreover, the phosphonate analogue Piv-P-MEP-G **8** of **5** was also designed. The phosphonate **8** has a one-carbon elongated side chain (C1′ to C5′) compared with that of adefovir **2**. Herein, we describe the results of the synthesis of **4-8** and evaluation of their anti-HBV activity.

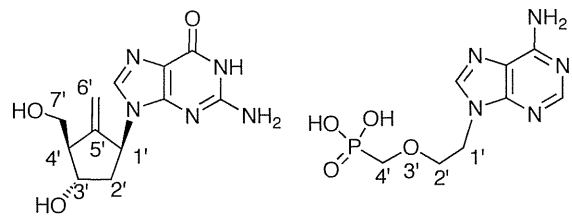

entecavir (**1**) adefovir (**2**)

Figure 1. Structure of entecavir (**1**) and adefovir (**2**).

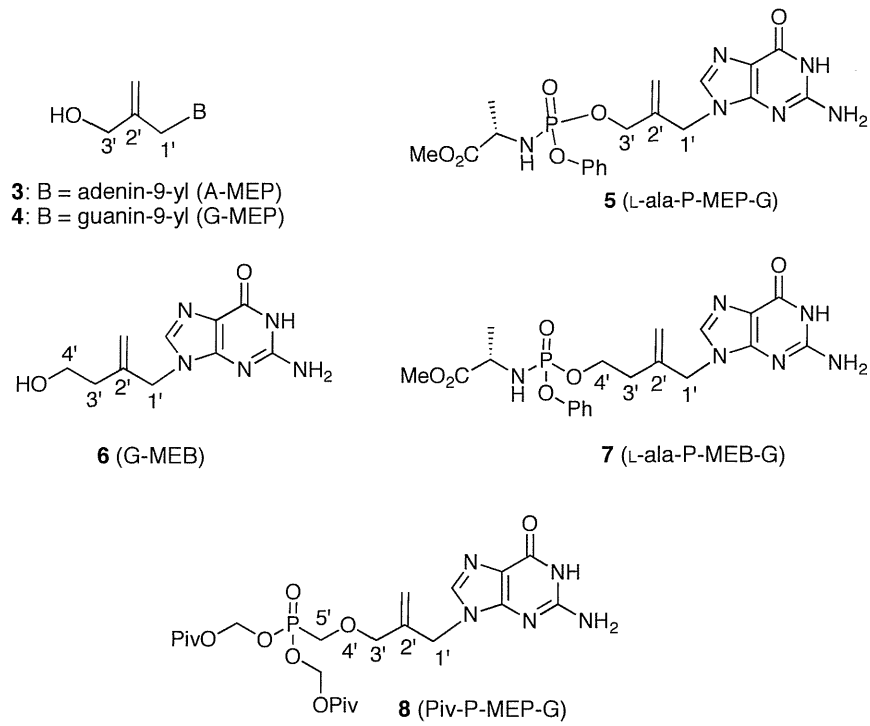

Figure 2. Structure of A-MEP (**3**) and the target molecules (**4-8**).

Results and Discussion

Chemistry

Initially, synthesis of G-MEP (**4**) was carried out (Scheme 1). Synthesis of the adenine counterpart **3** (A-MEP) of the target molecule **4** has been reported.[6] Therefore, according to the literature procedure, 2-methylenepropane-1,3-diol (**9**) was utilized as a starting material. Compound **9** was converted into 2-*O*-(*tert*-butyldimethylsilyloxymethyl)prop-2-en-1-ol (**10**). The literature procedure for the coupling of adenine with the acyclic moiety involved the mesylation of **10** followed by nucleophilic substitution of the respective mesylate with the nucleobase under the

basic reaction conditions. To reduce the synthetic steps to the target G-MEP **4**, Mitsunobu-type reaction of **10** with 2-*N*-acetyl-6-*O*-diphenylcarbamoylguanine (**11**)[7] was examined. Thus, when **10** was reacted with **11** in the presence of DIAD/Ph_3P in THF at 70 °C, the desired protected acyclopurine nucleoside **12** could be obtained in 53% yield. Removal of the protecting groups in the base moiety was carried out by treatment of **12** with ammonium hydroxide in methanol to give guanine derivative **13** in 88% isolated yield. In the HMBC spectra of **13**, the correlation between $C\underline{H}_2$-1′ / $\underline{C}$-4 and $C\underline{H}_2$-1′ / $\underline{C}$-8 was observed, by which **13** was assigned as N^9-isomer. Compound **13** was converted to MEP-G **4** in 33% yield by treating with Bu_4NF. Finally, **4** was transformed into the phosphoalaninate pro-drug **5** (16%) by reaction with methyl chlorophenylphosphoryl *P*→*N*-L-alaninate and *N*-mehtylimidazole in pyridine.[8]

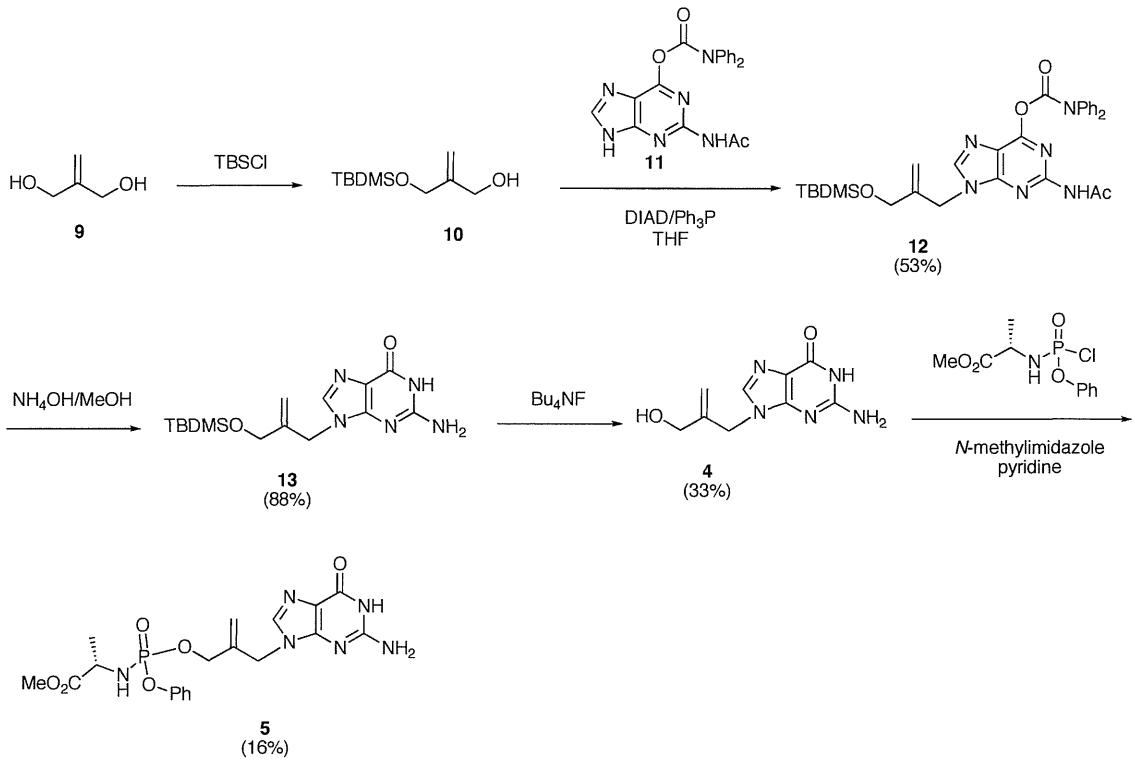

Scheme 1. Synthesis of G-MEP (**4**) and its monophosphate pro-drug L-ala-P-MEP-G (**5**)

Next, synthesis of G-MEB (**6**) was performed (Scheme 2). Initially, 4-(*tert*-butyldiphenylsilyloxy)-2-methylenebutan-1-ol (**16**) was prepared from **14** in 3 steps; 1) silylation of **13**, 2) epoxidation of the resulting silylated alkene, 3) β-elimination of the obtained epoxide **15** with diethylaluminium 2,2,6,6-tetramethylpiperidide.[9] When **16** was reacted with **11** under the above mentioned reaction conditions, the desired N^9-substituted **17** was obtained in 69% isolated yield as a single regio-isomer. Compound **17** was converted into **18** in 81% yield by ammonolysis in methanol and its HMBC spectra revealed the correlation

between CH_2-1′ / C-4 and CH_2-1′ / C-8. Desilylation of **18** gave G-MEB (**6**) in 60% yield. As described above for **4**, MEB-G **6** was transformed into phosphoralaninate pro-drug **7** in 57% yield.

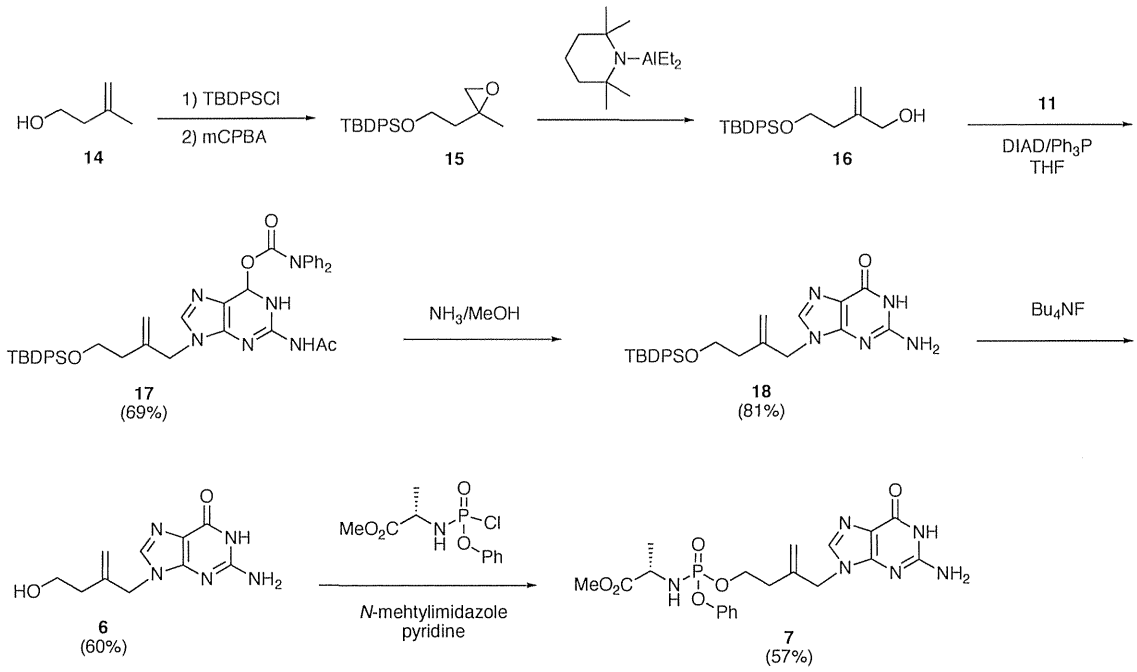

Scheme 2. Synthesis of G-MEB (**6**) and L-ala-P-MEB-G (**7**).

Finally, synthesis of the phosphonate analogue **8** of L-ala-P-MEB-G **7** was accomplished as illustrated in Scheme 3. Phosphonate alcohol **19** was prepared from **9** according to the published procedure.[6] Reaction of the alcohol **19** with **11** under the identical conditions for the synthesis of **17** gave the desired **20** in 62% isolated yield. Treatment of **20** with aqueous ammonia in methanol provided acycloguanine phosphonate derivative **21** in 54% yield and at this stage, the regiochemistry was